Cardiovasc Intervent Radiol
DOI 10.1007/s00270-007-9029-2

TECHNICAL NOTE

Contrast-Enhanced Abdominal Angiographic CT for Intra-abdominal Tumor Embolization: A New Tool for Vessel and Soft Tissue Visualization

Bernhard Christian Meyer · Bernd Benedikt Frericks · Thomas Albrecht · Karl-Jürgen Wolf · Frank Klaus Wacker

Abstract C-Arm cone-beam computed tomography (CACT), is a relatively new technique that uses data acquired with a flat-panel detector C-arm angiography system during an interventional procedure to reconstruct CT-like images. The purpose of this Technical Note is to present the technique, feasibility, and added value of CACT in five patients who underwent abdominal transarterial chemoembolization procedures. Target organs for the chemoembolizations were kidney, liver, and pancreas and a liposarcoma infiltrating the duodenum. The time for patient positioning, C-arm and system preparation, CACT raw data acquisition, and data reconstruction for a single CACT study ranged from 6 to 12 min. The volume data set produced by the workstation was interactively reformatted using maximum intensity projections and multiplanar reconstructions. As part of an angiography system CACT provided essential information on vascular anatomy, therapy endpoints, and immediate follow-up during and immediately after the abdominal interventions without patient transfer. The quality of CACT images was sufficient to influence the course of treatment. This technology has the potential to expedite any interventional procedure that requires three-dimensional information and navigation.

B. C. Meyer (✉) · B. B. Frericks · T. Albrecht · K.-J. Wolf · F. K. Wacker
Klinik und Hochschulambulanz für Radiologie und Nuklearmedizin, Campus Benjamin Franklin, Charité–Universitätsmedizin Berlin, Hindenburgdamm 30, 12200 Berlin, Germany
e-mail: bernhard.meyer@charite.de

Keywords Interventional radiology · Imaging guidance · Angiographic C-arm CT · Abdominal interventions · Chemoembolization.

Introduction

The safety of local chemotherapy and chemoembolization in the abdomen depends largely on accurate visualization of both the soft tissue and the vascular anatomy. The exact knowledge of the vessels that feed a tumor is essential for therapy that exclusively targets a tumor with only minimal collateral damage. This is especially important in patients who are treated for palliation rather than for cure. One way to control the catheter position for a targeted therapy is to perform CT angiography while injecting contrast through a catheter positioned in a vessel that feeds the tumor (IA-CTA) [1, 2]. However, moving patients from the angio to the CT table is time-consuming and presents the risk of catheter dislocation even in hybrid systems that combine a CT scanner and an angiography system in one suite [1]. In addition, such combination suites are controversial as far as performance, cost, and efficiency go.

Cone-beam volume CT, or angiographic C-arm CT (CACT), facilitates acquisition and reconstruction of CT-like images using a flat-panel angiography system without patient transfer. CACT allows a contrast resolution of 10 HU as well as a slice thickness and in-plane resolution of <1 mm. In cases of arterial embolization the combination of CACT and intra-arterial contrast injection through the catheter already in position can easily be performed without any patient movement.

The purpose of this Technical Note is to present the technique and assess the feasibility of abdominal CACT data acquisition and reconstruction as well as to evaluate the added value of CACT images for abdominal interventions.

Materials and Methods

The study was approved by the institutional review board, and written informed consent was obtained from each patient prior to the intervention. All patients were scheduled for transarterial chemoembolization (TACE). Three different abdominal interventions with different target organs were selected for this pilot study. The CACT was performed in the course of the intervention. Two attending radiologists assessed in consensus whether CACT images provided relevant information that changed the course of the interventional treatment.

Technique

All interventions were performed on a biplanar angiography system (AXIOM Artis dBA; Siemens Medical Solutions, Forchheim, Germany) equipped with a 30 × 40-cm flat-panel detector. The CACT runs were obtained using the 10s1k preset (DynaCT; Siemens Medical Solutions) with an acquisition time of 10 s, a total scan angle of 222°, a projection increment of 0.8°, a 1k-matrix, a zoom of 0, a field of view (FOV) of 48 cm, and a system dose per pulse of 0.36 mGy. The raw data sets from the angiographic C-arm system were sent to a dedicated external workstation (X-Leonardo; Siemens Medical Solutions) and reconstructions were performed to generate the CACT images. The volume data set produced by the workstation had a typical voxel size of 0.4 mm. For all reconstructions we used the ''bone smooth'' reconstruction kernel with a large FOV and artifact reduction as recommended by the manufacturer of the angiographic system for abdominal CACT images. Using these parameters, the time for CACT image reconstruction ranged between 3 min 40 s and 5 min 10 s. Immediately after reconstruction, the images were displayed on the external workstation as well as in the angiographic suite in three orthogonal planes. In addition, the data set was reformatted interactively using maximum intensity projections (MIPs) and multiplanar reconstructions (MPRs) with a slice thickness of 5 mm. Window and level settings could be adjusted individually during viewing and manipulation in orthogonal and oblique planes.

Patients

Patient 1

A 44-year-old man who suffered from an ocular melanoma was treated with radiotherapy 6 months prior to the intervention. An MRI (Magnetom Avanto 1.5T; Siemens Medical Solutions) was performed 3 weeks prior to the intervention consisting of T2-weighted turbospin echo (respiratory triggered; TR/TE, 2760/100 ms; slice thickness, 5 mm), T1-weighted gradient echo (breath-hold; TR/TE, 106/4.8 ms; slice thickness, 5 mm), and three-dimensional (3D) gradient echo sequences (TR/TE, 5.6/2.9 ms; slice thickness, 3 mm; acquired prior to and 15, 60, 120, and 600 s after injection of 0.2 ml/kg Gd-DTPA; Magnevist, Schering, Berlin), which revealed hepatic and renal metastasis (Fig. 1a). The patient was scheduled for TACE of his liver metastasis. In addition, selective chemoembolization of a renal metastasis that extended to the renal capsule was planned for pain management. A preinterventional CACT of the upper abdomen was performed in the portal-venous phase with a C-1 catheter in the superior mesenteric artery (SMA). The contrast agent (20 ml Iomeprol; Bracco, Milano, Italy) was diluted with 20 ml saline for an iodine concentration of 150 mg /ml and administered at a flow rate of 3 ml/s with an injection-to-scan delay of 20 s (Fig. 1b). The left kidney was catheterized and the artery that supplied the renal metastasis at the left upper pole was selectively embolized for pain treatment. To assess the perfusion defect in the left kidney after chemoembolization, an CACT run was performed (C-1 catheter in the left renal artery; 15 ml Iomeprol diluted with 15 ml saline, for an iodine concentration of 150 mg /ml; flow, 2.5 ml/s; delay, 3 s). The perfusion defect showed complete coverage of the metastasis (Figs. 1c and d) and the procedure was terminated. The patient was discharged 2 days after the procedure pain free without undergoing an additional contrast-enhanced multidetector-row helical CT (MDCT).

Patient 2

A 37-year-old women presented with a neuroendocrine tumor of the body of the pancreas and hepatic metastases that were diagnosed 2 weeks prior to the intervention on MDCT (Somatom Emotion 6, Siemens; arterial and portal-venous phase; collimation, 6 × 4 mm; 120 kV, 183 mA). Due to the age of the patient and the lack of other therapeutic options including surgery, transarterial chemotherapy was recommended by our institutional tumor board. To assess the feeding vessels of the tumor, digital subtraction angiograms of the celiac trunk and the SMA were obtained (Fig. 2c). A major tumor-feeding vessel was identified arising from the SMA. To confirm that this vessel was exclusively feeding the tumor, without any side branches going to the small bowel, an CACT run was performed (C-1 catheter in the SMA; 15 ml Iomeprol diluted with 30 ml saline, for an iodine concentration of 100 mg /ml; flow, 4 ml/s; delay, 3 s). MPR and MIP projections of the CACT images (Figs. 2d–f) showed both the branches of the SMA that fed the tumor and the opacified parenchyma of the tumor. Based on these images, a selective catheter position was obtained in the tumor-feeding SMA branch and local chemoembolization was performed using 80 mg of

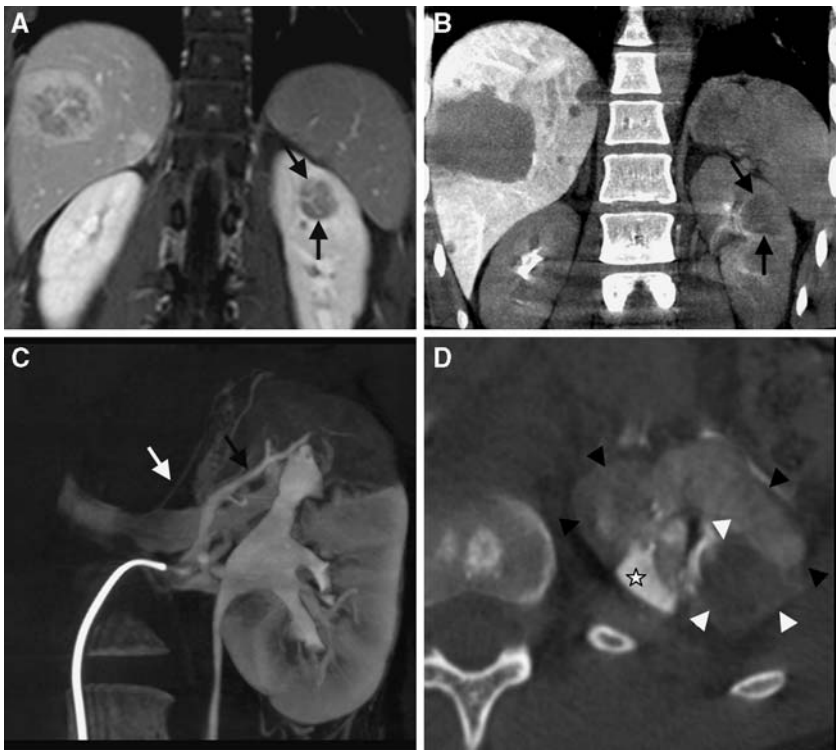

Fig. 1 Chemoembolization of a renal metastasis. **A** Coronal T1-weighted fat-saturated postcontrast MRI, acquired prior to the intervention, shows hepatic metastases and renal metastasis in the upper third of the left kidney (arrow). **B** CACT of the upper abdomen in the portal-venous phase. Disseminated hepatic metastases and renal metastasis in the upper third of the left kidney (arrow). **C**, **D** CACT images acquired after chemoembolization of the left kidney. The perfusion defect in the upper pole of the kidney can clearly be appreciated. A segmental artery feeding the upper pole is still opacified (black arrow). CACT allows differentiation of the perfusion defect (black arrowhead), metastasis (white arrowhead), and the normally perfused renal parenchyma (asterisk). Note the excellent visualization of the small left adrenal gland vein (white arrow)

cisplatin mixed with 450 mg of starch microspheres (Fig. 2g). The patient presented with moderate pain that was treated overnight, and she was discharged without further complications 2 days after the procedure.

Patients 3 and 4

A 72-year-old woman and a 68-year-old man both suffered from hepatocellular carcinoma diagnosed prior to the intervention by MDCT, contrast-enhanced ultrasound, and needle biopsy. The angiography performed prior to the TACE showed anatomical variants of the liver arteries. In both patients branches of the left gastric artery were feeding the left liver lobe. To further clarify the anatomy of the different branches coming off the left gastric artery (Fig. 3) that could not be comprehensively determined by one digital subtraction angiography (DSA) projection alone, and to visualize the liver lesions in relation to the hepatic arteries, we decided to perform an arterial and portal-venous CACT run in both patients (arterial run, C-1 catheter in the celiac trunc, 15 ml Iomeprol diluted with 30 ml saline for an iodine concentration of 100 mg/ml, 4 ml/s flow, 3 s delay; portal-venous run, C-1 catheter in the SMA, 15 ml Iomeprol diluted with saline for an iodine concentration of 150 mg /ml, 4 ml/s flow, 20 s delay). In the female patient, the CACT showed segmental partial thrombosis of the portal vein, which was initially not diagnosed on biphasic MDCT (Somatom Sensation 16, Siemens; arterial and portal-venous phase, 16 × 0.75-mm collimation, 1-mm slice thickness, 120 kV, 180 mA) acquired 1 day prior to the procedure, but was confirmed retrospectively after reviewing the MDCT images (Figs. 3a and b). To clarify the left hepatic artery anatomy, thin-slice MIP of the arterial phase CACT images was used, which facilitated not only the hepatic branches of the left gastric artery but also the branches that were feeding the stomach and the diaphragm (Figs. 3e and f). Therefore, the optimal catheter position could be determined without selective catheterization of these branches. Both patients tolerated TACE of the liver without any complications and were discharged 1 day after the procedure.

Patient 5

A 78-year-old man suffered from an abdominal liposarcoma that could not be completely resected during surgery.

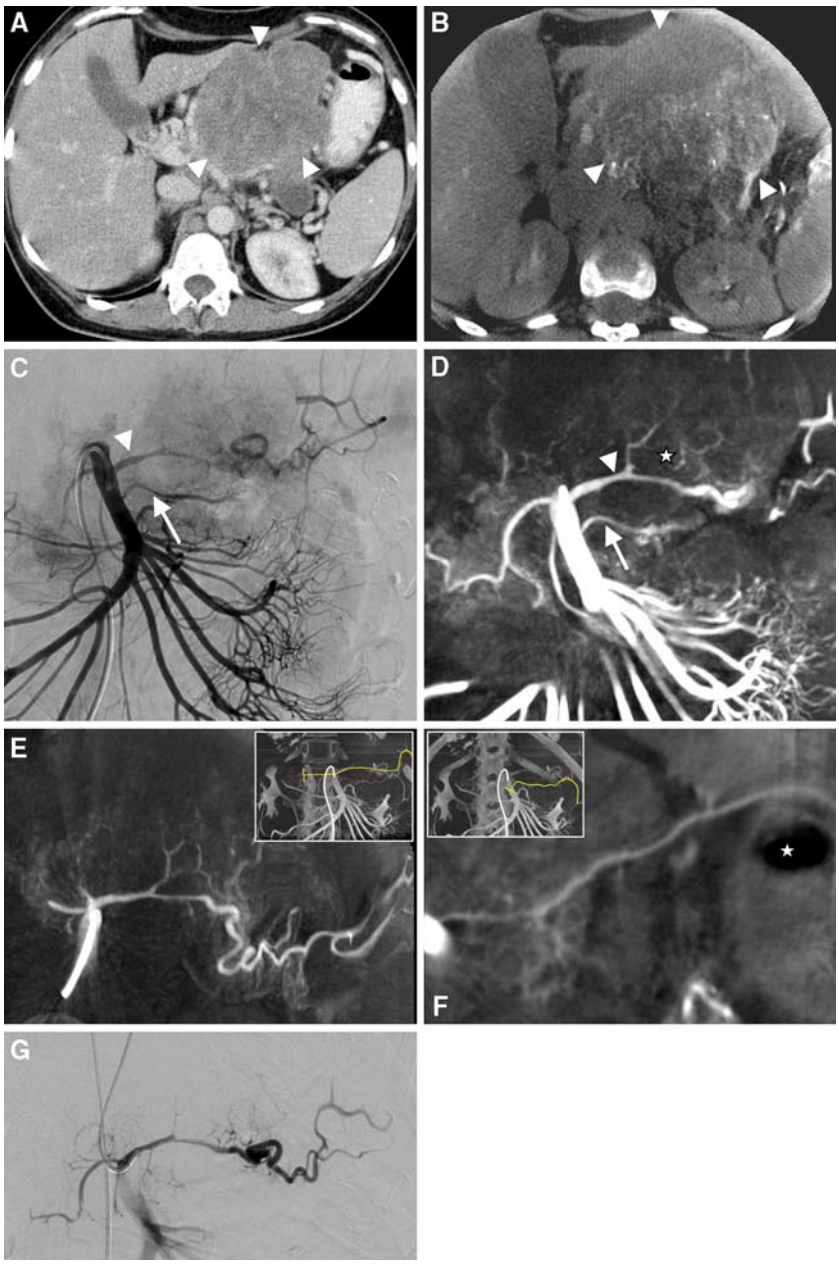

Fig. 2 Local chemotherapy of the pancreas. **A** MDCT of the abdomen 2 weeks prior to the local chemotherapy shows a large tumor mass in the pancreatic body (arrowhead). **B** Axial arterial CACT with the catheter located in the SMA. Inhomogeneous contrast enhancement of the pancreatic tumor (arrowhead). **C**, **D** DSA and coronal arterial CACT of the SMA showing the blood supply of the tumor. Two proximally arising branches of the SMA (arrowhead and arrow) are feeding the tumor. The position of the arteries in relationship to the tumor (asterisk) can be better appreciated with CACT (D). **E** On curved multiplanar reconstruction of the CACT images, the upper tumor-feeding artery can be identified as the inferior pancreatic artery (white arrowhead in C and D) with distal anastomoses to the splenic artery. **F** The curved multiplanar reconstruction along the second artery (white arrow in C and D) proves that this is the middle colic artery that extends to the left colonic flexure. **G** Selective DSA run with the catheter positioned in the inferior pancreatic artery that was selected for local chemotherapy

Ten weeks after resection, MDCT (Somatom Sensation 16, Siemens; arterial and portal-venous phase, 16×0.75-mm collimation, 1-mm slice thickness, 120 kV, 180 mA) revealed an abdominal mass in close proximity to the duodenum suggestive of duodenal wall infiltration (Fig. 4a). Systemic chemotherapy was started. During the first chemotherapy session intermittent GI bleeding was observed. A duodenoscopy showed bleeding ulcers that were related to direct tumor infiltration of the duodenal wall. In the first step, digital subtraction angiograms of the celiac trunk and the SMA were obtained, which were inconclusive for the identification of tumor-feeding vessels (Fig. 4e). To identify the tumor-feeding mesenteric branches that could not be comprehensively determined by one DSA projection alone and to visualize the tumor in relation to the feeding arteries, we decided to perform an arterial CACT run (C-1 catheter in the SMA, 15 ml Iomeprol diluted with 30 ml saline for an iodine concentration of 100 mg /ml, 4 ml/s flow, 3-s delay; Fig. 4c and d). With CACT, three arteries coming off the SMA could be identified that were feeding the tumor exclusively. After subsequent positioning of a microcatheter in these branches, embolization of the tumor was performed with microembospheres. Embolization was well tolerated. GI bleeding in the duodenum was not observed during endoscopy on the day after the intervention and systemic chemotherapy was continued.

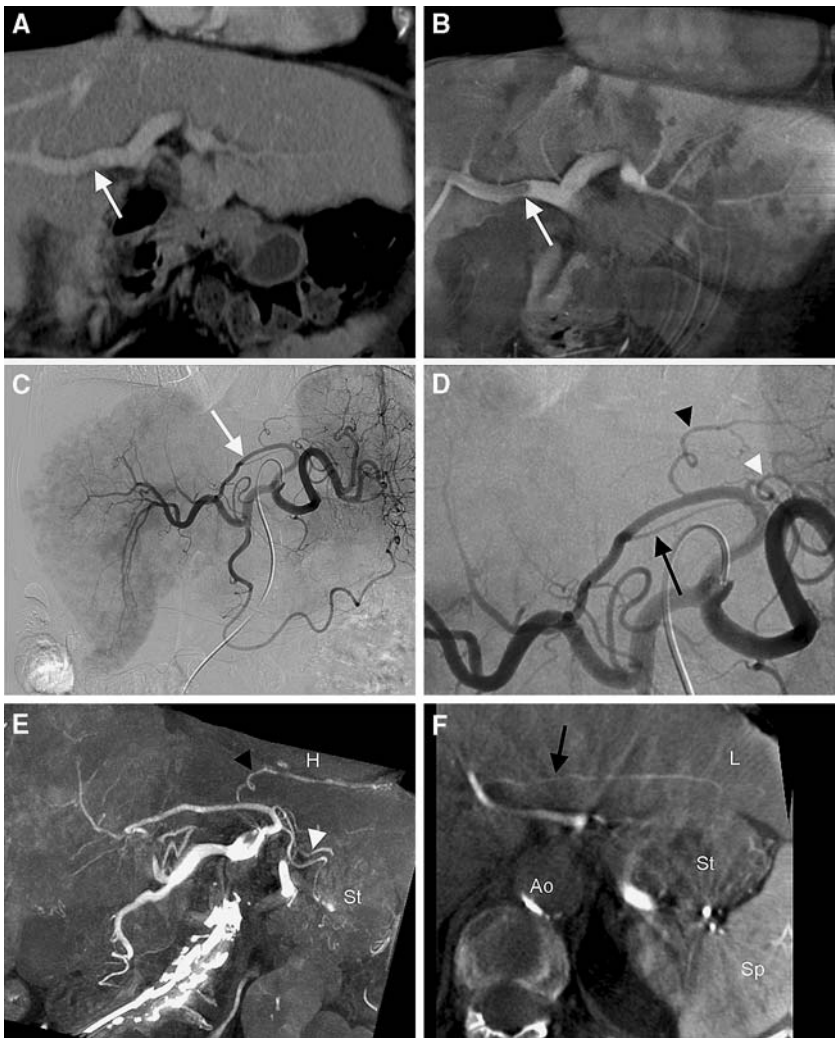

Fig. 3 TACE of the liver. **A**, **B** Coronal MPR (3 mm) of the MDCT (A) and the CACT (B), both in the portal-venous phase. The disseminated hepatic metastasis as well as the segmental partial thrombosis of the portal vein (arrow) can be better appreciated with CACT. **C** DSA shows the left hepatic artery feeding liver segments 2, 3, and 4 (arrow) coming off the prominent left gastric artery. **D** Enlarged view of the DSA shown in C. Clear classification of the three proximal side branches of the left gastric artery could not be achieved on a single projection. **E**, **F** Coronal curved MPR of the CACT, with simultaneous presentation of both the soft tissue and the arteries, facilitates clear identification of the gastric branches (white arrowhead in D and E), a phrenic branch (black arrowhead in D and E), and a hepatic branch (black arrow in D and F) feeding liver segments 2 and 3. Based on these findings, the catheter for chemoembolization of the left liver lobe was positioned at the arrowhead shown in C. St, stomach; Ao, aorta; L, liver; Sp, spleen; H, heart

Results

In this pilot study acquisitions of contrast-enhanced CACT runs were obtained for all patients without technical difficulties. The time to perform a single CACT study during an intervention ranged from 6 to 12 min. This includes patient positioning, C-arm and system preparation, data acquisition, and data reconstruction. CACT images provided additional findings that changed the course of the procedures as follows. In one patient, one segmental partial thrombosis of the portal vein was detected that was not initially diagnosed on MDCT but could be delineated when reviewing the images after obtaining the results of the portal-venous CACT images. In the last two cases, in which the vessel anatomy was essential to planning targeted treatment, MIP of the CACT images proved instrumental not only to understanding the three-dimensional anatomy but also to appreciating the relationship of the relevant soft tissue structures to the respective vessels. Most of the information CACT provides could also be obtained by performing additional DSA runs or selective catheterization of tumor-feeding or accessory arteries. However, it seems that based on our very limited experience so far, CACT might be able to provide the same information without the need to perform selective catheterization, which might require a microcatheter as well as extra time. In addition, CACT provides soft tissue information that is not provided by DSA alone. Although CACT images showed mild truncation and streaking artifacts in all patients and were not of the quality of conventional CT, they were sufficient to influence the course of the treatment in all cases.

Discussion

As long as 25 years ago, the advantages of both IA-CTA and CT during arterial portography (IA-CTAP), over conventional CT, were demonstrated [3, 4]. The basic principle of both methods relies on selective delivery of

Fig. 4 Embolization of a liposarcoma infiltrating the duodenum. **A**, **B** MDCT and CACT of the abdomen shows a large tumor (arrows) infiltrating the duodenum (asterisk). **C**, **D** MIP (15 mm; C) and MPR (5 mm; D) of the CACT in the arterial phase provides information on both feeding vessels and soft tissue of the tumor (arrowheads) and the surrounding structures. This enables clear-cut identification of two tumor-feeding arteries (white and black arrow). **E** DSA of the SMA shows multiple small branches, but conclusive identification of tumor-feeding vessels is not provided. **F** Selective angiogram proves successful embolization of one of the feeding vessels (white arrow; same vessel as in C, D, and E)

contrast material to the liver via the hepatic artery and the portal vein. This is achieved by placing an angiographic catheter with the tip in the hepatic artery or the SMA. Both methods can provide excellent conspicuity of hepatic tumors [4–11]. The benefit of IA-CTA was also reported for local arterial chemotherapy of nonresectable pancreatic tumors. In such cases, IA-CTA facilitates correct positioning of the catheter in the tumor-feeding vessel. Due to the fact that the arterial supply of the pancreas varies widely, this of the utmost importance in order to avoid adverse effects such as pain and necrosis due to bowel involvement [12]. Acquisition of CACT images using a flat-panel detector system offers increased spatial resolution over MDCT. High-contrast objects as small as 0.4 mm can be visualized. In combination with the higher contrast concentration due to intra-arterial contrast injection, this leads to highly improved visualization of smaller vessels compared to CTA acquired in a MDCT during intravenous administration of contrast medium (IV-CTA). However, the most important benefit of CACT is its unrestricted availability during any angiographic procedure, as in the same flat detector C-arm system both DSA and C-arm CT can be obtained interchangeably. Risky and time-consuming patient transfer from the angiography table to other imaging modalities such as MR or CT is not needed. Investment in costly hybrid systems that combine CT and angiography can be avoided [1].

Potential disadvantages of CACT include the increased amount of contrast agent, additional radiation exposure, and additional time required for setup, CACT run, and reconstruction. In our cases CACT provided detailed information on vascular anatomy. Thus additional oblique DSA runs were avoided. Based on our own limited experience with abdominal CACT as well as the first reports on neurointerventional applications [13], CACT was instrumental for complication management, therapy planning, and immediate follow-up and might replace postinterventional CT scans in selected cases. It remains to be seen if this compensates for the time, dose, and contrast agent used for CACT.

It is beyond the scope of this Technical Note to evaluate the impact of CACT on the tumor response or clinical outcome of the patients. We selected different abdominal tumors to present the technical feasibility and the potential usefulness for abdominal interventions. Further studies will be needed to define the merits of this device that combines CT and angiography in one system.

References

1. Hirai T, Korogi Y, Ono K, Maruoka K, Harada K, Aridomi S, Takahashi M (2001) Intraarterial chemotherapy or chemoembolization for locally advanced and/or recurrent hepatic tumors: evaluation of the feeding artery with an interventional CT system. Cardiovasc Intervent Radiol 24(3):176–179
2. Sze DY, Razavi MK, So SK, Jeffrey RB Jr (2001) Impact of multidetector CT hepatic arteriography on the planning of chemoembolization treatment of hepatocellular carcinoma. AJR 177(6):1339–1345
3. Prando A, Wallace S, Bernardino ME, Lindell MM Jr (1979) Computed tomographic arteriography of the liver. Radiology 130(3):697–701
4. Helmberger H, Bautz W, Vogel U, Lenz M (1993) [CT arterioportography in the spiral technic for the demonstration of liver metastases]. Rofo 158(5):410–415
5. Matsui O, Takashima T, Kadoya M, Ida M, Suzuki M, Kitagawa K, Kamimura R, Inoue K, Konishi H, Itoh H (1985) Dynamic computed tomography during arterial portography: the most sensitive examination for small hepatocellular carcinomas. J Comput Assist Tomogr 9(1):19–24
6. Chezmar JL, Bernardino ME, Kaufman SH, Nelson RC (1993) Combined CT arterial portography and CT hepatic angiography for evaluation of the hepatic resection candidate. Work in progress. Radiology 189(2):407–410
7. Kanematsu M, Hoshi H, Imaeda T, Murakami T, Inaba Y, Yokoyama R, Nakamura H (1997) Detection and characterization of hepatic tumors: value of combined helical CT hepatic arteriography and CT during arterial portography. AJR 168(5):1193–1198
8. Kanematsu M, Oliver JH 3rd, Carr B, Baron RL (1997) Hepatocellular carcinoma: the role of helical biphasic contrast-enhanced CT versus CT during arterial portography. Radiology 205(1):75–80
9. Matsui O, Kadoya M, Kameyama T, et al. (1991) Benign and malignant nodules in cirrhotic livers: distinction based on blood supply. Radiology 178(2):493–497
10. Matsui O, Kadoya M, Suzuki M, Inoue K, Itoh H, Ida M, Takashima T (1983) Work in progress: dynamic sequential computed tomography during arterial portography in the detection of hepatic neoplasms. Radiology 146(3):721–727
11. Murakami T, Oi H, Hori M, Kim T, Takahashi S, Tomoda K, Narumi Y, Nakamura H (1997) Helical CT during arterial portography and hepatic arteriography for detecting hypervascular hepatocellular carcinoma. AJR 169(1):131–135
12. Maurer CA, Borner MM, Lauffer J, Friess H, Z'Graggen K, Triller J, Buchler MW (1998) Celiac axis infusion chemotherapy in advanced nonresectable pancreatic cancer. Int J Pancreatol 23(3):181–186
13. Heran NS, Song JK, Namba K, Smith W, Niimi Y, Berenstein A (2006) The utility of DynaCT in neuroendovascular procedures. Am J Neuroradiol 27(2):330–332